JOURNAL OF PROPULSION AND POWER
Vol. 26, No. 4, July–August 2010

Flow Control in a Compressor Cascade at High Incidence

Simon Evans*
Worcester Polytechnic Institute, Worcester, Massachusetts 01609
Howard Hodson† and Tom Hynes‡
University of Cambridge, Cambridge, England CB3 0DY, United Kingdom
and
Christian Wakelam§
Universität der Bundeswehr München, 85577 Neubiberg, Germany

DOI: 10.2514/1.48054

Flow control has been applied on the suction surface of blades within a compressor cascade to remove a turbulent boundary-layer separation that occurs at an incidence of 12.5°. Vortex generator jets and boundary-layer suction through discreet holes have each been applied to the suction surface to push the point of separation from 54% chord to the trailing edge. Corner separations also occurring at this incidence have been controlled by means of endwall suction. The mixed-out stagnation-to-stagnation pressure loss coefficient was measured in each case tested. The measured loss coefficients were used, together with an endwall suction-loss coefficient and a boundary-layer control loss coefficient, to estimate the total loss coefficient for a compressor blade with a representative aspect ratio of 3.5. For such a blade, endwall suction and vortex generator jets on the suction surface were found to yield a 20% reduction in the total loss coefficient relative to the uncontrolled case. Endwall suction, together with boundary-layer suction on the suction surface, was found to yield a 33% reduction in the total loss coefficient. Flow control was also applied to the suction surface at a range of incidences from 0 to 15.5°. Only boundary-layer suction was able to achieve a loss reduction at 15.5°.

Nomenclature

A	=	area, m^2
b	=	blade span, m
C_μ	=	injected momentum coefficient
$\dot{m}$	=	mass flow rate, kg/s
p_0	=	stagnation pressure, Pa
s	=	blade pitch, m
V	=	velocity, m/s
Y	=	loss coefficient,
α	=	flow angle, °
ρ	=	density, kg/m^3

Subscripts

a	=	averaged over full span
END	=	endwall
j	=	jet
MEAS	=	measured
p	=	profile
s	=	suction
1	=	upstream
2	=	downstream

I. Introduction

VARIABLE inlet guide vanes (IGVs) and variable stator vanes extend the range of operation of a compressor by increasing their stagger angle when the compressor operates offdesign. The increased stagger angle allows the stator blades to receive the flow from upstream rotor blade rows at a reasonable incidence. It also increases the exit flow angles from the stator and IGV blade rows, such that incidence onto the following fixed-stagger rotor blades is not so high as to cause flow separation from the suction surfaces of the airfoils. The disadvantage of this system, however, is the complexity of the variable geometry and the weight of the drive system required to operate it. These systems can weigh as much as two passengers on a large twin-engine wide-body aircraft. It is, therefore, of interest to develop a virtual variable-guide vane system in which variable stagger is replaced by actuation on the blades themselves. This actuation is required to control the flow direction as the engine moves offdesign and the blades experience increasing levels of incidence. As the incidence increases, the flow will tend to separate from the suction surfaces of the airfoils. This separation must be reduced or eliminated, so as to minimize the blockage and loss it creates. Flow control has been explored extensively for the purpose of separation control, both for external and internal flows, and so is explored here for this purpose.

Another potential application of flow control in compressors is on highly loaded blades that would separate under design conditions without control. The increased loading that flow control allows the blades to be designed with means that fewer blades are needed for the same turning, or that increased turning is achieved for the same number of blades. Both translate into a reduction in weight and part count.

Flow control has been applied for separation control in axial compressors in the past by Culley et al. [1] and Kirtley et al. [2]. Both used streamwise blowing, reenergizing what appears to be laminar boundary layers by direct momentum addition. The work presented here, however, applies flow control to delay the turbulent open type of separation that is more typical of compressor blades at high incidence.

Vortex generator jets have been shown to create streamwise vortices in turbulent boundary layers with no pressure gradient [3,4], as well as laminar boundary layers in the presence of a pressure gradient [5]. They have also been used by Bons et al. [6,7] and Volino [8] to control laminar separations on low-pressure turbine blades. The vortices created by vortex generator jets reenergize the boundary

Received 9 November 2009; revision received 19 March 2010; accepted for publication 19 March 2010.

*Assistant Professor, Department of Mechanical Engineering, 100 Institute Road; sevans@wpi.edu.
†Professor of Aerothermal Technology, Whittle Laboratory, Department of Engineering, 1 JJ Thomson Avenue.
‡Reader, Whittle Laboratory, Department of Engineering, 1 JJ Thomson Avenue.
§Research Associate, Institute for Jet Propulsion.

layer by transporting high-momentum freestream fluid into the inner boundary layer and transporting low-momentum fluid from the inner boundary layer away from the wall. It is this use of freestream momentum to reenergize the boundary layer that allows for a lower level of injected momentum to achieve the same level of control as a streamwise jet [9]. Further mass flow reduction may be achieved by pulsing the jet. Pulsing at prescribed frequencies also allows natural frequencies within the flow to be excited and generates more mixing than is achievable with a steady jet, due to the presence of a starting vortex with each pulse.

Evans et al. [10] have explored the application of vortex generator jets in a flow simulating that on the suction surface of a compressor blade. A turbulent separation occurring at 70% suction surface length was successfully removed with a steady jet blowing at a jet velocity equal to the inlet flow velocity, achieving a reduction in the mixed-out stagnation-to-stagnation pressure loss coefficient of 36%. Evans et al. [10] also explored pulsed blowing in this application, finding that pulsed blowing only achieved the same level of loss reduction as steady blowing with an increased maximum jet velocity and a pulse frequency corresponding to 130 kHz in the intermediate pressure compressor of a full-size aeroengine. The challenges associated with achieving such a jet on a real blade led Evans et al. [10] to recommend steady blowing over pulsed blowing in this application.

Suction is another technique that has been investigated for separation control in compressors [11,12]. By sucking low-momentum fluid from the near-wall region, a fuller boundary-layer velocity profile is promoted and the onset of separation delayed. Schuler [13] explored boundary-layer suction in a fan stage, increasing loading and, therefore, pressure rise.

In addition to the loss associated with a separated boundary layer, high incidence also serves to increase the extent of the hub-corner separation that occurs in rotors and shrouded stators. Hub-corner separations are the result of an interaction between the flow on the suction surface of the blade and the secondary flow on the hub, which is overturned by the cross-passage pressure gradient. This overturning brings low-momentum fluid from the hub boundary layer into the hub-corner region. If the blade is highly loaded, this low stagnation pressure fluid is not able to negotiate the pressure rise, and a hub-corner separation occurs. This increases blockage and loss production and can affect compressor stability.

Similar behavior has been widely observed on the endwalls of linear compressor cascades. Gbadebo et al. [14] show that the thickness of the separated flow region increases as the incidence of the blade is increased. Blockage and loss increase accordingly.

If the loss and blockage at high incidence are to be reduced, control of the separating suction surface boundary layer must be accompanied by control of the endwall corner separations. A number of approaches for the control of corner separations have been explored, including tip gaps [15–17], passive devices [18], and endwall suction [17,19]. Peacock [19] appears to be the first to have suggested the latter approach, recommending slots in the endwalls next to the suction surface corner that extend from 50% chord to the trailing edge. Gbadebo [17] also applied endwall suction, successfully removing the corner separation and achieving an increase in blade loading and a more uniform exit flow.

In this paper, both steady vortex generator jets and boundary-layer suction are explored for control of the separating, turbulent boundary layer that occurs on the suction surface of the blades of a linear compressor cascade at high incidence. The coupling between boundary-layer control and control of the endwall corner separations is also explored. Endwall control is performed by means of endwall suction.

II. Experimental Facilities and Procedures

The study described in this paper was performed in a linear cascade of seven blades located at the exit of a low-speed continuous blower-type wind tunnel at the Whittle Laboratory. The cascade has variable incidence, allowing the inlet flow angle to be varied from 36.5 to 52°. The blade profile was designed by MTU Aero Engines to have the same pressure distribution at low speed as a typical compressor blade at high speed. A schematic of the cascade is shown in Fig. 1. A mesh screen is located downstream of the cascade to pressurize the test section to a pressure greater than atmospheric pressure. This allows the upstream boundary layers on the ceiling, floor, and sidewalls to be bled off through slots connected to the atmosphere. Table 1 gives the main parameters characterizing the cascade. Periodicity of the stagnation-to-stagnation pressure loss coefficient was achieved to within 0.004 across the middle three wakes of the cascade. The turbulence intensity at inlet was measured as 0.5%.

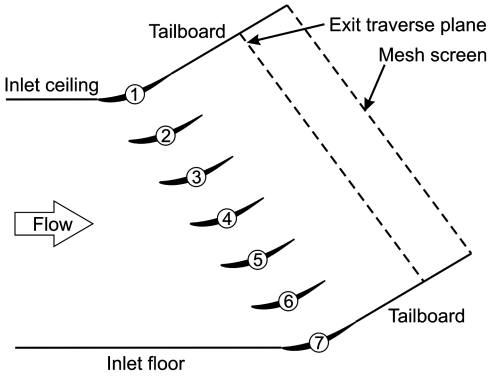

Fig. 1 Schematic of linear compressor cascade.

Each blade contains one row of jet holes located at 54% chord (61% suction surface length) on the suction surface. The jet holes are 4 mm in diameter, pitched at 30° to the surface, and skewed at 60° to the freestream direction, as recommended by Evans et al. [10]. The pitch and skew angles are defined in Fig. 2. All the jets are skewed in the same direction.

The jet hole diameter of 4 mm is 16% of the measured local displacement thickness δ^* and 46% of the measured local boundary-layer thickness δ_{99} at the jet hole location. This is slightly smaller than the holes used by Bons et al. [6,7] and Volino [8]. The holes are spaced by 8.125 jet diameters.

The jets are supplied with air from the laboratory air system via external pipes and channels within the blades. The internal geometry of a blade is shown in Fig. 3. In addition to seven blades with this internal geometry, three hollow blades were also made. In these blades, additional jet holes were inserted at 29.5% chord (35% suction surface length). These holes were used in those experiments for which separation occurred upstream of 54% chord.

The stagnation-to-stagnation pressure profile loss coefficient Y_p measured at midspan was used to evaluate the effectiveness of flow control in the cascade. This is defined in Eq. (1) as the sum of a measured loss coefficient $Y_{\text{meas},p}$ calculated from stagnation pressure measurements taken across the wake, a jet loss coefficient Y_j that accounts for the mixing of the injected jet fluid with the mainstream fluid, and a suction-loss coefficient Y_s for the cases with boundary-layer suction. The measured loss coefficient is defined in Eq. (2) in terms of the mixed-out stagnation pressure p_{02} derived from measurements taken at the midspan, one chord downstream of the trailing edge of the middle blade (blade 4 in Fig. 1). A Neptune probe was used for these measurements. This probe combines a three-hole probe and a cone probe for static pressure measurement on a single stem. The two probes are 1 in. apart. This probe is based on a design by Sieverding et al. [20]. The jet loss coefficient Y_j and suction-loss coefficient Y_s are defined in Eqs. (3) and (4) in terms of the jet mass

Table 1 Characterization of cascade

Parameter	Value
Chord	325 mm
Solidity	1.53
Aspect ratio	1.9
Design inlet flow angle	36.5°
Reynold's number	0.5×10^6

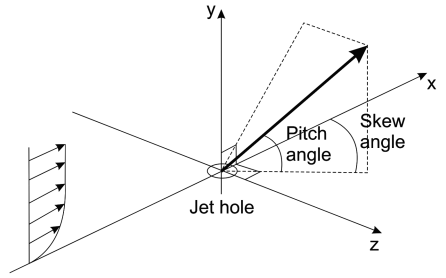

Fig. 2 Angle definitions for vortex generator jets.

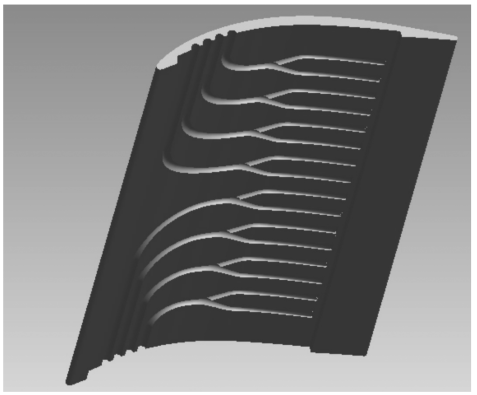

a)

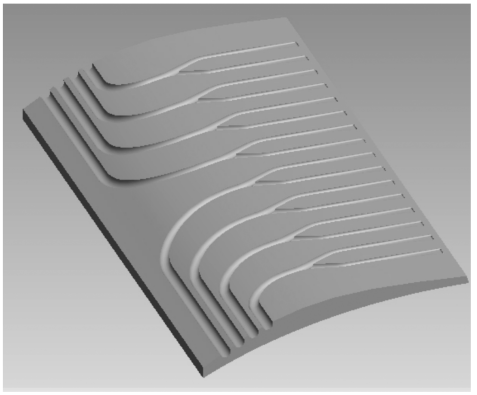

b)

Fig. 3 CAD model of compressor cascade blade showing internal geometry: a) suction surface part and b) pressure surface part.

flow rate $\dot{m}_j$ and boundary-layer suction mass flow rate $\dot{m}_s$ (which has a negative sign), respectively. These mass flow rates are defined as the total for a single blade (i.e., for 16 jet holes). The mass flow rate $\dot{m}_2$ is defined as the sum of $\dot{m}_1$, $\dot{m}_j$, and $\dot{m}_s$, where $\dot{m}_1$ is the mass flow rate entering a single passage of the cascade:

$$Y_p = Y_{\text{meas},p} + Y_j + Y_s \tag{1}$$

$$Y_{\text{meas},p} = \frac{p_{01} - p_{02}}{(1/2)\rho V_1^2} \tag{2}$$

$$Y_j = \left(\frac{\dot{m}_j}{\dot{m}_2}\right)\left(\frac{p_{0j} - p_{02}}{(1/2)\rho V_1^2}\right) \tag{3}$$

$$Y_s = -\left(\frac{\dot{m}_s}{\dot{m}_2}\right)\left(\frac{p_{0s} - p_{02}}{(1/2)\rho V_1^2}\right) \tag{4}$$

In addition to the profile loss coefficient Y_p, the stagnation-to-stagnation mixed-out loss coefficient was also averaged over the full blade span. This area loss coefficient Y_a is defined in Eq. (5) as the sum of a measured loss coefficient $Y_{\text{meas},a}$, a jet loss coefficient $Y_{j,a}$, a boundary-layer suction-loss coefficient $Y_{s,a}$, and an endwall suction-loss coefficient $Y_{s,\text{end}}$. The measured loss coefficient $Y_{\text{meas},a}$ is defined in Eq. (6) in terms of a stagnation pressure p_{02a} averaged over the full span. The jet loss coefficient $Y_{j,a}$ and boundary-layer suction-loss coefficient $Y_{s,a}$ are also defined in terms of this pressure, in Eqs. (7) and (8), respectively. The endwall suction-loss coefficient is defined in Eq. (9) in terms of the endwall suction mass flow rate $\dot{m}_{s,\text{end}}$ and stagnation pressure $p_{0s,\text{end}}$:

$$Y_a = Y_{\text{meas},a} + Y_j + Y_s + Y_{s,\text{end}} \tag{5}$$

$$Y_{\text{meas},a} = \frac{p_{01} - p_{02a}}{(1/2)\rho V_1^2} \tag{6}$$

$$Y_j = \left(\frac{\dot{m}_j}{\dot{m}_2}\right)\left(\frac{p_{0j} - p_{02a}}{(1/2)\rho V_1^2}\right) \tag{7}$$

$$Y_s = -\left(\frac{\dot{m}_s}{\dot{m}_2}\right)\left(\frac{p_{0s} - p_{02a}}{(1/2)\rho V_1^2}\right) \tag{8}$$

$$Y_{s,\text{end}} = -\left(\frac{\dot{m}_{s,\text{end}}}{\dot{m}_2}\right)\left(\frac{p_{0s,\text{end}} - p_{02a}}{(1/2)\rho V_1^2}\right) \tag{9}$$

The jet velocity may be normalized by either the inlet or local freestream velocity. The injected momentum coefficient C_μ is also used for nondimensionalization of the jet velocity, and it is recommended by Luedke et al. [9] as the appropriate parameter for scaling pressure recovery in a diffuser. The injected momentum coefficient is used here and is defined in Eq. (10) as the ratio of the injected to the inlet momentum flux. The jet area A_j is defined as the total jet area for a single blade (i.e., 16 jet holes):

$$C_\mu = \frac{2A_j}{bs\cos(\alpha_1)}\left(\frac{V_j}{V_1}\right)^2 \tag{10}$$

III. Experimental Results

A. Uncontrolled Performance at 12.5° Incidence

Figure 4 shows the midspan isentropic surface velocity distribution calculated from static pressure measurements taken at midspan for an incidence of 12.5°. Despite the high incidence, oil flow visualization showed no evidence of separation at midspan. The constant velocity from 65% chord to the trailing edge, shown in Fig. 4, is not a separation but an artifact of stream-tube convergence caused by corner separations and the geometry over the aft portion of the blade.

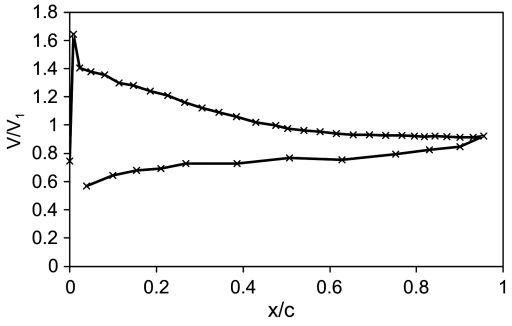

Fig. 4 Isentropic surface velocity distribution with no boundary-layer or endwall control. Incidence = 12.5°. Midspan AVR = 1.07.

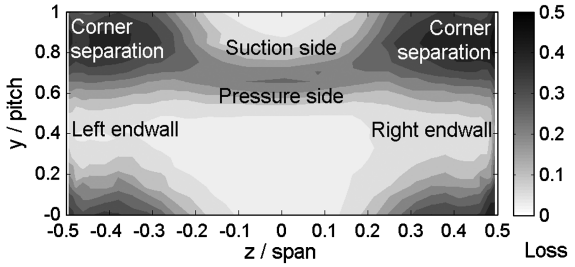

Fig. 5 Measured loss contours one chord downstream of the cascade with no boundary-layer or endwall control. Incidence = 12.5°. Midspan AVR = 1.07.

The midspan profile loss coefficient Y_p is 0.034. The midspan axial velocity ratio (AVR) is 1.07. The midspan AVR is defined as the ratio of the mass-averaged midspan axial velocity at exit to the inlet axial velocity.

Figure 5 shows contours of the mixed-out loss coefficient measured one chord downstream of the trailing edge of blade 4, also for an incidence of 12.5°. The loss contours span one blade pitch and the full blade span. The wake is shown with the blade suction surface above and the pressure surface below.

Figure 5 shows large loss cores downstream of the corners between the suction surface and the endwalls that dominate the flow. These extend over almost 25% of the blade span on each side, and they are consistent with the presence of large corner separations, the presence of which was confirmed using surface flow visualization.

The blockage resulting from the loss cores shown in Fig. 5 causes spanwise convergence of the stream tube as the flow passes from the leading edge of the blade to the trailing edge, reducing the diffusion at midspan and raising the midspan AVR to 1.07. It is this reduced diffusion at midspan that prevents boundary-layer separation despite the high incidence. The absence of separation results in a thin wake at midspan, as shown in Fig. 5.

The mixed-out loss coefficient averaged over the full span Y_a is 0.132. This is significantly higher than the midspan profile loss coefficient Y_p, and it is consistent with the large loss cores shown in Fig. 5.

The flow shown in Figs. 4 and 5 confirmed the need for endwall control. Until the corner separations were controlled, the application of flow control to the suction surface boundary layer was ineffective at reducing the loss, as the midspan boundary layer was not separated.

B. Endwall Control

Endwall suction was applied through suction slots opened on the endwall, along the corner between the aft suction surface and the endwall. These slots extend from 40% chord (45% suction surface length) to the trailing edge. A mass flow rate of 0.7% of the inlet mass flow rate was sucked off to achieve an AVR of one, measured at midspan, for the incidence of 12.5°.

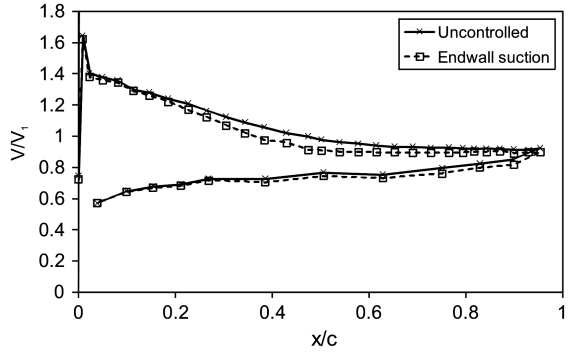

Fig. 6 Isentropic surface velocity distributions with no boundary-layer or endwall control (uncontrolled) and with endwall suction. Incidence = 12.5°. With endwall suction, midspan AVR = 1.0, $\dot{m}_s/\dot{m}_1 = 0.7\%$.

The isentropic surface velocity distribution measured on the midspan is shown in Fig. 6 for this case. The case with no boundary layer or endwall control is also shown, for reference. With the application of endwall suction, separation was identified at 54% chord. The midspan profile loss coefficient Y_p is 0.069. with a precision error of ±0.0035. This loss represents an increase of 102%, relative to the uncontrolled case. Gbadebo et al. [14] also reports an increase in the profile loss coefficient with the application of endwall control, although the experiments reported by Gbadebo et al. [14] were not performed at an incidence for which the suction surface boundary layer separated.

Loss contours measured downstream of the cascade with endwall suction are shown in Fig. 7. The loss cores shown in the suction surface/endwall corners in Fig. 5 have been removed, and the midspan wake is thickened. Removal of the corner separations has removed the convergence of the stream tube observed without endwall control, yielding a midspan AVR of one. This has resulted in a rise in the adverse pressure gradient at the midspan, causing boundary-layer separation and the thickened midspan wake evident in Fig. 7.

The loss coefficient averaged over the full span Y_a is 0.087 in this case. This represents a loss reduction relative to the uncontrolled case of 34%. It includes the endwall suction-loss component $Y_{s,\mathrm{end}}$, which contributes 0.014. The measured loss coefficient $Y_{\mathrm{meas},a}$ contributes 0.073. In addition to reducing the loss coefficient averaged over the full span, endwall control has caused a midspan separation, creating the opportunity for further loss reduction by means of boundary-layer separation control on the blade suction surface.

C. Boundary-Layer Control: Vortex Generator Jets

Flow control was applied to the suction surface boundary layer in the form of steady vortex generator jets located at 54% chord: the observed separation location for the case with endwall suction and no boundary-layer control. The impact of control on the midspan profile loss coefficient Y_p is shown as a function of the injected momentum coefficient C_μ in Fig. 8. The ratio of injected to inlet mass flow rate is also shown. Two cases of endwall suction are shown. These cases are described as fixed and tuned endwall suction. With fixed endwall

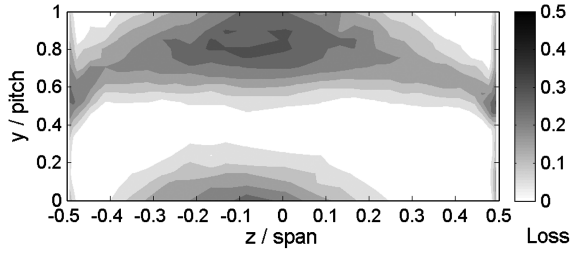

Fig. 7 Measured loss contours one chord downstream of the cascade with endwall suction. Incidence = 12.5°. Midspan AVR = 1.0.

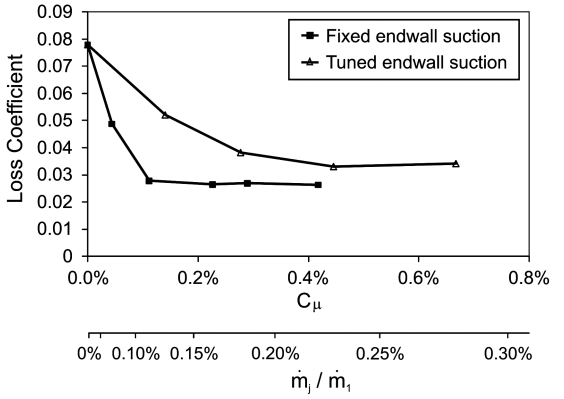

Fig. 8 Midspan profile loss coefficient plotted against injected momentum coefficient. Incidence = 12.5°.

suction, the same level of endwall suction is applied with boundary-layer control, as was found necessary to give a midspan AVR of one with no boundary-layer control. With tuned endwall suction, however, additional endwall suction is applied in order to keep the midspan AVR equal to one when the boundary-layer control is applied.

With fixed endwall suction, the midspan profile loss coefficient Y_p is shown to decrease rapidly as the injected momentum is increased, reaching 0.026 at an injected momentum coefficient of 0.1%. This is a loss reduction of 62% relative to the case with no boundary-layer control. No further loss reduction was achieved with a further increase in the injected momentum coefficient.

Measured loss contours for the case with boundary-layer control with an injected momentum coefficient of 0.4% are shown in Fig. 9 for the case with fixed endwall suction. Consistent with the midspan profile loss reduction, shown in Fig. 8, the midspan wake is greatly thinned relative to the case with no boundary-layer control, shown in Fig. 7. In addition to a thinned midspan wake, however, Fig. 9 contains a large loss core on the left-hand side of the blade passage. This coincides with an aggravated corner separation on this side of the blade that yields an increase in the midspan AVR to a value of 1.05 for all injected momentum coefficients greater than 0.1%.

The variation of the midspan AVR with the injected momentum coefficient follows the variation of the midspan profile loss coefficient, shown in Fig. 8, suggesting that the blockage generated in the left-hand corner is driven by the state of the boundary layer rather than by the momentum injected into it. The asymmetry of the flow shown in Fig. 9, however, suggests a link to the spanwise component of jet momentum introduced by the jets, which are all skewed toward the left-hand endwall.

The presence of a corner separation means that some stream-tube convergence occurs in all of the controlled cases shown for fixed endwall suction in Fig. 8. This offloads the midspan boundary layer to some extent, effectively helping to delay the midspan separation.

The loss coefficient averaged over the full span Y_a for the case with an injected momentum coefficient of 0.4% is 0.096. Although this is 27% lower than the loss coefficient in the uncontrolled case, it is actually an increase of 10% relative to the case with no boundary-layer control. This increase is a result of an 8% increase in the measured loss coefficient $Y_{\text{meas},a}$ coupled with the addition of a jet loss term Y_j of 0.002.

To remove the aggravated corner separation shown on the left of Fig. 9, the level of suction on the left-hand endwall was increased. The additional mass flow sucked from the flow passage was determined as that required for the midspan AVR to equal one. This was done for each value of injected momentum coefficient tested. The resulting midspan profile loss coefficient Y_p is plotted under the legend of tuned endwall suction in Fig. 8.

As the injected momentum was increased, Fig. 8 shows that the midspan profile loss coefficient again reached a threshold beyond which no further loss reduction was achieved by a further increase of the injected momentum coefficient. This threshold occurs at an injected momentum coefficient of 0.44%. This is notably higher than the threshold observed in the profile loss coefficient generated with boundary-layer control and fixed endwall suction. The minimum profile loss coefficient Y_p of 0.033 is also slightly higher than the minimum profile loss coefficient measured with fixed endwall suction. This minimum represents a 52% reduction in the midspan profile loss coefficient relative to the case with no boundary-layer control.

The mass flow removed from the endwalls is an important element in the endwall suction-loss coefficient, which contributes to the loss coefficient averaged over the full span. The mass flow rate sucked through the left-hand endwall was increased from 0.35% of the inlet mass flow rate, with no boundary-layer control to 1.00% for all cases with boundary-layer control. The mass flow rate sucked through the right-hand endwall remained constant at 0.35%.

A number of isentropic surface velocity distributions are shown in Fig. 10 for various levels of injected momentum coefficient for the case of tuned endwall suction. Also shown is the case with no boundary-layer control. Figure 10a shows the full distribution from the leading edge of the blade to the trailing edge, while Fig. 10b shows the detail over the aft suction surface, a region identified with a zoom box in Fig. 10a. Figure 10 shows that control with an injected momentum coefficient of 0.14% achieved neither noticeable delay of separation nor any increase in diffusion. However, with an injected momentum coefficient of 0.27%, separation has been delayed to 80% chord and the trailing-edge velocity has decreased, increasing diffusion on the aft suction surface. An increase in the injected momentum coefficient to 0.44% caused the separation to be pushed off the trailing edge and a further increase in the diffusion. For the highest two levels of injected momentum coefficient shown, 0.44 and 0.66%, the distributions are similar downstream of 70% chord. In the region of 50% chord, however, the higher injected momentum coefficient data shows a higher velocity, indicating less diffusion over the forward portion of the blade and more over the aft portion. The overall diffusion achieved between the suction peak and trailing edge is, however, almost identical in the two cases. This is consistent with Fig. 8, which shows the same value of the midspan profile loss coefficient at these two conditions.

Measured loss contours are shown over the full span in Fig. 11 for the case with tuned endwall suction and boundary-layer control with an injected momentum coefficient of 0.44%. The thinned wake at midspan extends across nearly 80% of the span. The loss core shown on the left-hand side of Fig. 9 has been removed. The loss coefficient averaged over the full span Y_a is 0.100. The measured loss coefficient

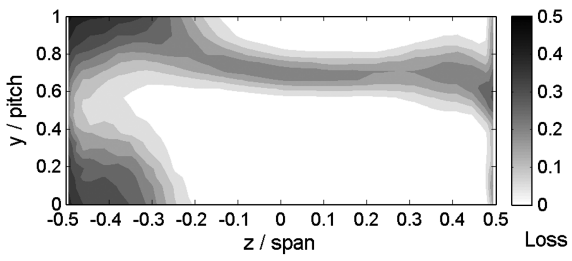

Fig. 9 Measured loss contours one chord downstream of cascade with boundary-layer control and fixed endwall suction. $C_\mu = 0.4\%$. Incidence = 12.5°. Midspan AVR = 1.05, $\dot{m}_s/\dot{m}_1 = 0.76\%$.

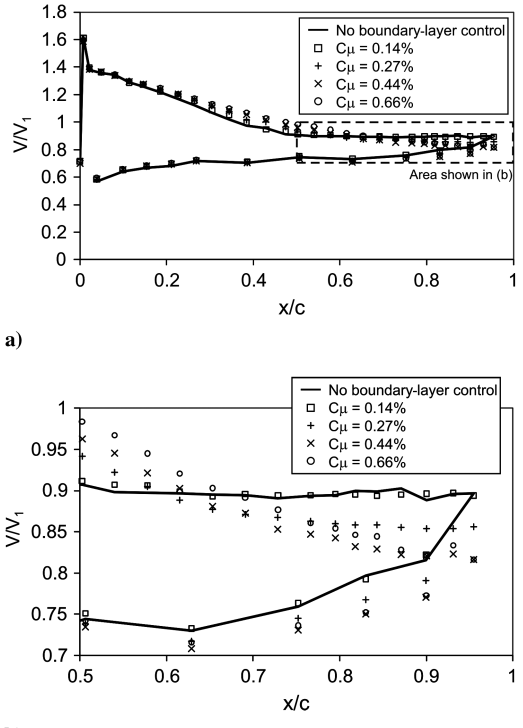

Fig. 10 Isentropic surface velocity distributions with tuned endwall suction and boundary-layer control. Incidence = 12.5°.

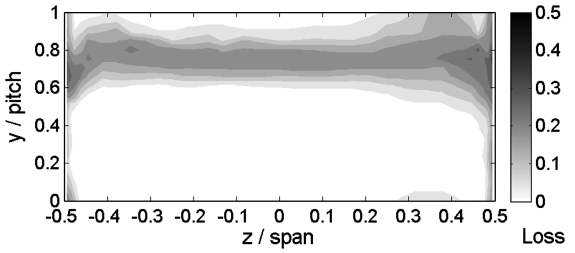

Fig. 11 Measured loss contours one chord downstream of the cascade with boundary-layer control and fixed endwall suction. $C_\mu = 0.44\%$. Incidence = 12.5°. Midspan AVR = 1.0, $\dot{m}_s/\dot{m}_1 = 1.4\%$.

averaged over the full span $Y_{\text{meas},a}$, however, is 0.053. This low value of $Y_{\text{meas},a}$ is consistent with the thin, uniform wake shown in Fig. 10. The endwall suction-loss coefficient $Y_{s,\text{end}}$ is 0.044. It is this term that brings the total loss coefficient Y_a to a value that is higher than that in the case with no boundary-layer control.

The removal of the corner separation and the blockage associated with it explains the increased injected momentum required to achieve the minimum profile loss coefficient Y_p, shown in Fig. 8, relative to the case with fixed endwall suction. With no stream-tube contraction, the diffusion required of the midspan boundary layer is not reduced, as in the case with fixed endwall suction. With no help from the corner separation, a higher level of injected momentum is required to achieve control.

D. Blowing over a Range of Incidence

The analysis described in Sec. III.C was repeated at various incidence angles extending from 0 to 15.5°, corresponding to inlet flow angles ranging from the design inlet flow angle of 36.5 to 52°. The midspan AVR was forced to equal one by means of endwall suction in all cases, both with and without boundary-layer control. In the cases with boundary-layer control, the midspan AVR was set by means of tuned endwall suction, as described in Sec. III.C.

At an incidence of 0°, the flow diffuses from 18.5% chord on the suction surface without any boundary-layer separation. The isentropic surface velocity distribution at 0° of incidence is shown in Fig. 12. As the incidence was increased to 6.5°, the boundary layer still remained attached. At 10.5° of incidence, however, the boundary layer separated at approximately 87% chord. This separation moved upstream to 54% chord at 12.5° of incidence, as shown in Fig. 6. At 15.5° of incidence, the point of separation moved further upstream to 43% chord. The isentropic surface velocity distribution for 15.5° of incidence is shown in Fig. 13.

The midspan profile loss coefficient Y_p is plotted against incidence in Fig. 14. The profile loss coefficient with no boundary-layer control is shown as a solid line. The influence of boundary-layer control is shown for injected momentum coefficients of 0.3 and 0.5%. Jets located at 54% chord were used at all incidence angles except 15.5°. At an incidence of 15.5°, the boundary layer separates upstream of this location, and so the blades with jet holes located at 29.5% chord were used. These holes are 5.5% of the suction surface length upstream of the point of separation measured at 15.5° of incidence. Only three blades have the upstream jet holes, and so the remaining

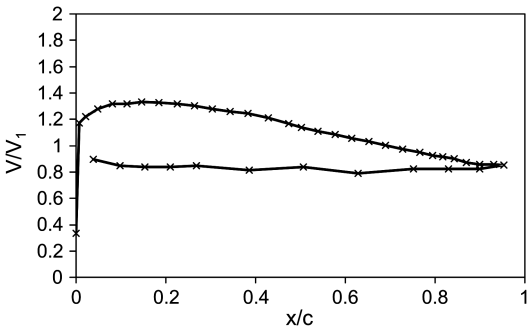

Fig. 12 Isentropic surface velocity distribution with endwall suction. Incidence = 0°. Midspan AVR = 1.0, $\dot{m}_s/\dot{m}_1 = 0\%$.

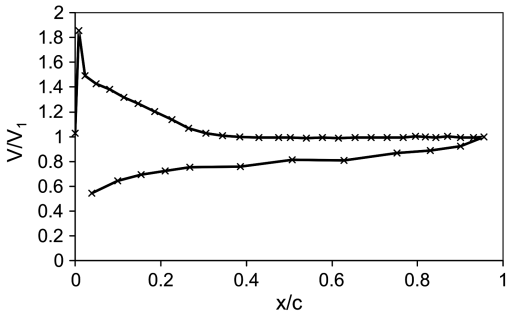

Fig. 13 Isentropic surface velocity distribution with endwall suction. Incidence = 15.5°. Midspan AVR = 1.0, $\dot{m}_s/\dot{m}_1 = 0.5\%$.

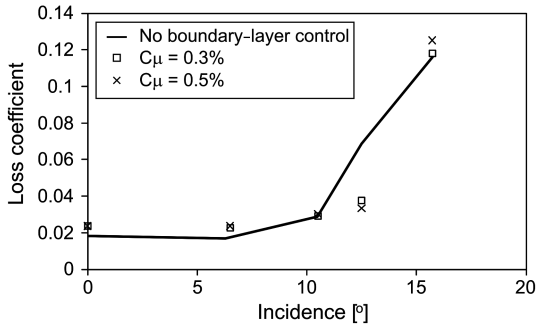

Fig. 14 Profile loss coefficient plotted against incidence for various levels of boundary-layer control. Endwall control by tuned endwall suction.

four blades in the cascade were used with jets issuing from the downstream holes located at 54% chord. The three blades with holes at 29.5% chord were located in the center of the cascade, including the center blade downstream of which wake measurements were taken, and those above and below it. By blowing the same mass flow rate through the other jet holes, a common injected mass flow rate was maintained in each passage.

At all incidence angles below 10.5°, boundary-layer control is shown to increase the midspan profile loss coefficient. For these cases, the boundary layer was not separated, and so the jets just added mixing loss. At an incidence of 10.5°, control yielded no change in the loss coefficient. At an incidence of 12.5°, a significant loss reduction was achieved with control, as has been discussed in Sec. III.C. As the incidence was increased to 15.5°, however, a loss reduction was no longer achieved, either with 0.3% injected momentum coefficient or 0.5%. This reveals a limit in the effectiveness of vortex generator jets to control the turbulent separation occurring on the suction surface of this blade.

It is not clear to what extent this result was impacted by the presence of jets located upstream of separation on only the center three blades. The fact that control was not achieved on these blades means that the blockage in all passages is, however, likely to be consistent. This implies that the inconsistency in jet hole location had a minimal impact in this case.

E. Boundary-Layer Control: Suction

Boundary-layer control was also applied by means of suction. Boundary-layer suction was performed using the same geometry described above for blowing with vortex generator jets. Although slots have been widely studied in this application, discreet holes have the advantage of not damaging the structural integrity of the blades to the same degree as slots. It was, therefore, believed reasonable to consider suction through the existing holes.

For an incidence of 12.5°, steady suction was applied through the jet holes located at 54% chord. Endwall suction was applied at the level necessary to yield a midspan AVR of one.

The midspan profile loss coefficient Y_p is plotted against the mass flow rate sucked from the suction surface of the blade in Fig. 15. The

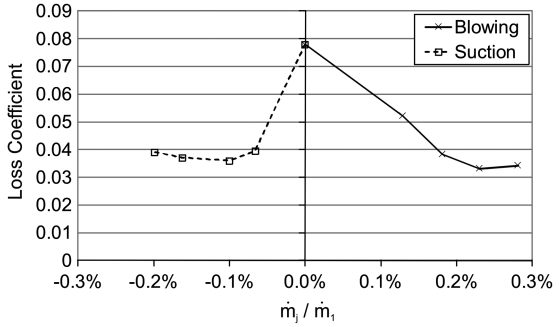

Fig. 15 Midspan profile loss coefficient plotted against control mass flow rate normalized by inlet mass flow rate. Endwall control by suction. Incidence = 12.5°.

sucked mass flow rate is shown as a negative jet mass flow rate. This loss coefficient includes the suction loss resulting from boundary-layer control Y_s. Also shown is the midspan profile loss coefficient with blowing and tuned endwall suction, also shown in Fig. 8. Horizontal grid lines have been added to the figure to facilitate comparison of the data.

Figure 15 shows that similar levels of loss reduction were achieved with boundary-layer suction as with blowing. The mass flow rate that was sucked from the boundary layer to achieve this level of loss reduction was 0.1% of the inlet mass flow rate. This corresponds to a velocity in the jet holes equal to 40% of the cascade inlet velocity. This mass flow rate is notably smaller than the 0.23% required to achieve the same loss reduction with blowing.

The minimum profile loss coefficient achieved with suction was 0.036, a 46% reduction relative to the case with no boundary-layer control. This is slightly higher than the value of 0.033 that was achieved with blowing. With blowing, the streamwise vortices created by the vortex generator jets are able to mix the boundary layer over the whole aft portion of the blade. In the case of suction, the control technique operates to remove low-momentum fluid only at the point of application. Some additional loss is, therefore, expected to be created as the boundary layer negotiates that portion of the blade suction surface downstream of the point of actuation.

The suction mass flow rate required to yield a midspan AVR of one with boundary-layer suction was the same as that required to yield a midspan AVR of one with no boundary-layer control on the suction surface. No additional suction was required from either endwall, as was the case with blowing, neither was any spanwise flow induced. This is a significant benefit of this approach.

Loss contours measured one chord downstream of the cascade are shown in Fig. 16 for the case with 0.17% of the inlet mass flow rate sucked from the boundary layer. This corresponds to a velocity in the jet holes equal to 60% of the cascade inlet velocity. These contours show that the boundary layer is controlled across the full span, confirming the absence of corner separations.

The loss coefficient averaged over the full span Y_a is 0.075 for this case. The endwall suction-loss term contributes 17% of this total, while the boundary-layer suction-loss term contributes 5%. This loss coefficient is lower than both the loss coefficient of 0.100 achieved with blowing and tuned endwall suction and the loss coefficient of 0.096 achieved with blowing and fixed endwall suction.

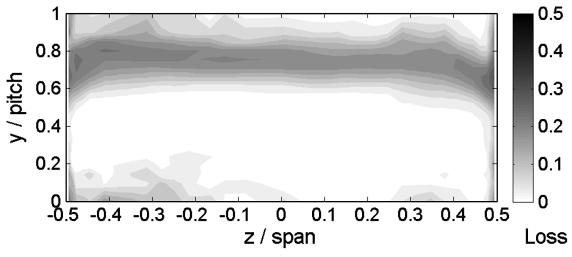

Fig. 16 Measured loss contours one chord downstream of the cascade with boundary-layer and endwall suction. $C_\mu = 0.23\%$. Incidence= 12.5°. Midspan AVR = 1.0. Endwall suction $\dot{m}_s/\dot{m}_1 = 0.7\%$.

F. Suction over a Range of Incidence

It was shown in Sec. III.D that only limited separation is observed at an incidence of 10.5° and that no separation is observed below this incidence. For this reason, control with suction was investigated at only 12.5° of incidence, as detailed in Sec. III.E, and at 15.5° of incidence. At this latter incidence, blowing with vortex generator jets was shown in Sec. III.D to not be effective at achieving any loss reduction. Suction at this incidence was performed through the same holes used for blowing: located at 29.5% chord, 5.5% suction surface length upstream of separation at this incidence.

The midspan profile loss coefficient Y_p is shown as a function of the mass flow rate sucked from the boundary layer in Fig. 17. Also shown are the results for blowing through the same jet holes. In all cases, the midspan AVR is one. As with Fig. 15, horizontal grid lines have been added to facilitate comparison of the data.

Figure 17 shows the slight loss increase that blowing yielded at this incidence (as shown in Fig. 14.) With suction, however, some loss reduction is evident. For a suction mass flow rate of 0.28%, the midspan profile loss coefficient Y_p is 0.096. This is 17% lower than measured in the case with no boundary-layer control. This suggests that, although the streamwise vortices created with blowing are not able to delay separation at this incidence, some separation delay is achievable with suction. This was also the highest suction mass flow rate tested, suggesting that greater loss reduction may be possible with increased levels of boundary-layer suction.

G. Correcting for Aspect Ratio

The aspect ratio of the cascade blade is 1.9. This is low, relative to an early stage intermediate compressor stator blade, for which 3.5 is more typical. The loss coefficient averaged over the span of a blade with an aspect ratio of 3.5 $Y_{a,3.5}$ can be estimated from the loss coefficient averaged over the cascade span Y_a and the midspan profile loss Y_p, using Eq. (11):

$$Y_{a,3.5} = Y_p + Y_j + Y_s + \tfrac{1.9}{3.5}(Y_a - Y_p + Y_{s,\text{end}}) \qquad (11)$$

The loss coefficient estimated for a blade with an aspect ratio of 3.5 is shown in Fig. 18 for a number of cases, all with an incidence of 12.5°. The loss coefficient is broken down into the estimated measured loss coefficient, the estimated endwall suction-loss coefficient, and the estimated boundary-layer control loss coefficient (either the jet loss coefficient Y_j or, in the case of boundary-layer suction, the boundary-layer suction-loss coefficient Y_s).

The loss coefficient $Y_{a,3.5}$ estimated for the uncontrolled case is 0.087. The application of endwall suction yields a 9% decrease in this loss coefficient to 0.079. This is much lower than the 34% loss reduction seen with the cascade blade. The reason is the relatively larger contribution of the midspan profile loss, which is high, since the midspan boundary layer is separated.

The application of blowing with vortex generator jets and no change in the endwall suction yields a further decrease in the loss coefficient $Y_{a,3.5}$ to 0.064. This is 26% lower than the loss coefficient in the uncontrolled case. The cost in terms of the jet loss coefficient is 0.002, while endwall suction contributes 0.008.

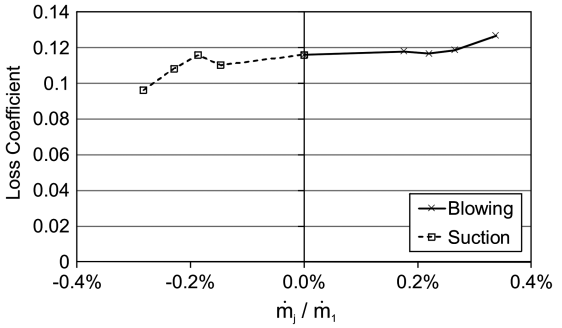

Fig. 17 Midspan profile loss coefficient plotted against control mass flow rate normalized by inlet mass flow rate. Endwall control by suction. Incidence = 15.5°.

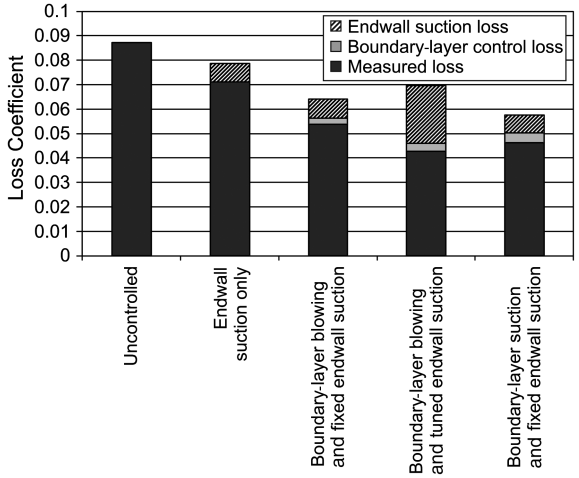

Fig. 18 Breakdown of loss coefficient averaged over the full span under various conditions of endwall and boundary-layer control. Incidence= 12.5°. Aspect ratio = 3.5. In cases with boundary-layer control, $C_\mu = 0.4\%$.

Increasing the endwall suction to remove the aggravated endwall corner separation occurring with fixed endwall suction yields an increase in the loss coefficient $Y_{a,3.5}$ to 0.070. This is still 20% lower than in the uncontrolled case. The measured loss coefficient has, in fact, been reduced to a value 50% lower than in the uncontrolled case. However, only some of this loss reduction is realized when the large endwall suction-loss coefficient of 0.024 is added.

The case with boundary-layer suction is also shown in Fig. 18. The loss coefficient $Y_{a,3.5}$ is 0.058. As with the cascade blade, this case has the lowest loss coefficient, 33% lower than in the uncontrolled case. This is despite having a higher measured loss coefficient than in the case with boundary-layer blowing and tuned endwall suction. The reason for the lower total loss coefficient is the lower endwall suction-loss term. This is possible because of the absence of an aggravated corner separation on the left-hand endwall in this case.

The stator blade row in a full-size aeroengine would be expected to have smaller corner separations than those seen in a cascade, due to the presence of inlet skew. Inlet skew can result from secondary flow in the rotor, a moving hub in the case of unshrouded stators or, simply, the change in frame of reference from the rotating frame to the stationary frame combined with variation of velocity magnitude in the hub boundary layer in the rotating frame. This inlet skew is generally in the direction of positive local incidence, toward the pressure surface of the blade. The inlet skew therefore tends to oppose overturning of the endwall flow, reducing the size of the corner separations. The influence of the corner separations in a blade row in a full-size aeroengine is therefore likely to be overpredicted by the loss coefficients averaged over the full span of a cascade blade, even with a representative aspect ratio.

Since the midspan loss coefficient is only slightly lower with suction than with blowing, and the loss coefficient averaged over the full span of a blade with a representative aspect ratio has a loss coefficient 0.012 lower with suction than with blowing, it must be concluded that suction is the approach recommended by these results. The achievement of some loss reduction with suction at the higher incidence of 15.5°, but not with blowing, adds weight to this conclusion.

With the above results recommending the application of flow control (particularly boundary-layer suction) to a compressor, it is worth considering how the implementation of a flow control system would impact the weight and cost of the compressor. The implementation of boundary-layer flow control and endwall suction requires design modifications to be made to the stator row to which control is applied, as well as the casing and hub of the compressor. High-pressure air is available at downstream stages in the compressor, and modifications to the secondary air system would allow it to be delivered to the blades. The same applies to suction air, if the air sucked from the endwalls and suction surface boundary layers is to be dumped into an upstream stage. Changes to the secondary air system do not necessarily yield increases in weight, but neither do they necessarily lead to decreases in weight. Furthermore, steady flow control applied to the boundary layer of stator blades means that material must be removed from the blades to create internal ducting to deliver air to or from the jet holes. The reduction in strength that this would cause may, however, yield a need for an alternative blade material, which may be both heavier and more costly than that currently in use. It is, therefore, difficult to estimate the weight addition that a flow controlled blade row would effect without a more detailed design being performed. The authors, however, believe it fair to assume that an increase in weight due to such a system would not be so large as to offset the benefits described in Sec. I.

As for the cost of implementation of the flow control system, this would largely come from the manufacturing costs associated with the internal geometry required in the stator blades and from the cycle impact of the application of control. The latter impact requires a rigorous cycle study to be performed, incorporating the additional downstream bleed required in the case of boundary-layer blowing, as well as the suction air dumped upstream of the flow-controlled stage. Such a study is the subject of ongoing work.

IV. Conclusions

Boundary-layer control by means of steady vortex generator jets has been shown to remove separation on the suction surface of a compressor cascade blade at 12.5° of incidence. When averaged over the full span and corrected to represent a blade with a representative aspect ratio, the measured loss coefficient is reduced by 50% relative to the uncontrolled blade. Properly accounting for the loss associated with the endwall suction required to control corner separations present at this incidence yields a reduction in the total loss coefficient of 20% relative to the uncontrolled case. Boundary-layer suction, however, yields a total loss reduction relative to the uncontrolled case of 33%. The poorer performance of blowing, when measured in terms of the total loss coefficient, is a result of the additional suction required to control the aggravated corner separation that forms as a result of the spanwise flow induced by blowing through skewed jets.

Extension of the investigation performed at 12.5° of incidence to a wide range of incidences revealed that no benefit was achieved by applying control to a boundary layer that did not exhibit separation. Furthermore, flow control by vortex generator jets was found to be limited in the extent of the separation that it was able to control, within the range of jet velocities tested. Although the steady vortex generator jets were able to effectively control the boundary-layer separation occurring at 12.5° of incidence, they were not able to control the boundary-layer separation occurring at an incidence of 15.5°. Boundary-layer suction at this incidence was, however, shown to yield a reduction in the profile loss coefficient of 17% relative to the case with no boundary-layer control.

Acknowledgments

This project was supported by funding under the Sixth Research Framework Program of the European Union, project ADVACT (advanced actuation concepts), contract number 502844. The work was performed at the Whittle Laboratory, University of Cambridge, United Kingdom. The excellent standards and support of the technical staff at the Whittle Laboratory are also acknowledged.

References

[1] Culley, D. E., Bright, M. M., Prahst, P. S., and Strazisar, A. J., "Active Flow Separation Control of a Stator Vane Using Surface Injection in a Multistage Compressor Experiment," NASA Glenn Research Center TM 2003-212356, 2003.

[2] Kirtley, K. R., Graziosi, P., Wood, P., Beacher, B., and Shin, H.-W., "Design and Test of an Ultra-Low Solidity Flow-Controlled Compressor Stator," *Proceedings of ASME Turbo Exposition*, American Society of Mechanical Engineers, GT2004-53012, New York, 2004, pp. 1–12.

[3] Compton, D. A., and Johnston, J. P., "Streamwise Vortex Production by Pitched and Skewed Jets in a Turbulent Boundary Layer," *AIAA*

Journal, Vol. 30, No. 3, March 1992, pp. 640–647.
doi:10.2514/3.10967

[4] Khan, Z. U., and Johnston, J. P., "On Vortex Generating Jets," *International Journal of Heat and Fluid Flow*, Vol. 21, No. 5, 2000, pp. 506–511.
doi:10.1016/S0142-727X(00)00038-2

[5] Hansen, L., and Bons, J. P., "Flow Measurements of Vortex Generator Jets in Separating Boundary Layer," *Journal of Propulsion and Power*, Vol. 22, No. 3, 2006, pp. 558–566.
doi:10.2514/1.13820

[6] Bons, J. P., Sondergaard, R., and Rivir, R. B., "The Fluid Dynamics of LPT Blade Separation Control Using Pulsed Jets," *Proceedings of ASME Turbo Expo*, American Society of Mechanical Engineers, New York, 2001, pp. 1–10.

[7] Bons, J. P., Sondergaard, R., and Rivir, R. B., "Turbine Separation Control Using Pulsed Vortex Generator Jets," *Journal of Turbomachinery*, Vol. 123, No. 2, 2001, pp. 198–206.
doi:10.1115/1.1350410

[8] Volino, R. J., "Separation Control on Low-Pressure Turbine Airfoils Using Synthetic Vortex Generator Jets," *Journal of Turbomachinery*, Vol. 125, No. 4, 2003, pp. 765–777.
doi:10.1115/1.1626686

[9] Luedke, J., Graziosi, P., Kirtley, K., and Cerretelli, C., "Characterization of Steady Blowing for Flow Control in a Hump Diffuser," *AIAA Journal*, Vol. 43, No. 8, Aug. 2005, pp. 1644–1652.
doi:10.2514/1.12797

[10] Evans, S. W., Hodson, H. P., Hynes, T. P., Wakelam, C. T., and Hiller, S.-J., "Controlling Separation on a Simulated Compressor Blade Using Vortex Generator Jets," 4th Flow Control Conference, AIAA Paper 2008-4317, Seattle, WA, June 2008.

[11] Reijnen, D. P., "Experimental Study of Boundary Layer Suction in a Transonic Compressor," Ph.D. Thesis, Massachusetts Inst. of Technology, Cambridge, MA, 1997.

[12] Merchant, A., "Aerodynamic Design and Performance of Aspirated Airfoils," *Proceedings of ASME Turbo Expo*, American Society of Mechanical Engineers, New York, 2002, pp. 1–11.

[13] Schuler, B. J., "Experimental Investigation of an Aspirated Fan Stage," Ph.D. Thesis, Massachusetts Inst. of Technology, Cambridge, MA, 2001.

[14] Gbadebo, S. A., Cumpsty, N. A., and Hynes, T. P., "Three-Dimensional Separations in Axial Compressors," *Proceedings of ASME Turbo Expo*, American Society of Mechanical Engineers, New York, June 2004, pp. 1–13.

[15] Dean, R. C., Jr., "The Influence of Tip Clearance on Boundary Layer Flow in a Rectilinear Cascade," Massachusetts Inst. of Technology Rept. 27-3, 1954.

[16] Lakshminarayana, B., and Horlock, J. H., "Leakage and Secondary Flows in Compressor Cascade," Aeronautical Research Council Rept. 3483, 1967.

[17] Gbadebo, S. A., "Three-Dimensional Separations in Compressors," Ph.D. Dissertation, Department of Engineering, Univ. of Cambridge, Cambridge, England, U.K., June 2003.

[18] Hergt, A., Meyer, R., and Müller, M. W., "Loss Reduction in Compressor Cascades by Means of Passive Flow Control," *Proceedings of ASME Turbo Expo*, American Society of Mechanical Engineers, New York, June 2008, pp. 1–12.

[19] Peacock, R. E., "Boundary-Layer Suction to Eliminate Corner Separation in Cascades of Aerofoils," Aeronautical Research Council Rept. 3663, 1971.

[20] Sieverding, C., Maretto, L., Lehthaus, F., and Lawaczeck, O., "Design and Calibration of Four Probes for Use in the Transonic Turbine Cascade Testing," Von Karmen Institute for Fluid Dynamics TN 100, Rhode-St-Genèse, Belgium, 1974.

A. Prasad
Associate Editor